

See discussions, stats, and author profiles for this publication at: <https://www.researchgate.net/publication/295100982>

The hydraulics of a vertical slot fishway: A case study on the multi-species Vianney-Legendre fishway in Quebec, Canada

Article *in* Ecological Engineering · May 2016

DOI: 10.1016/j.ecoleng.2016.01.032

CITATIONS

0

READS

194

5 authors, including:



Abul Basar M. Baki
Ecofish Research Ltd.
17 PUBLICATIONS 68 CITATIONS

[SEE PROFILE](#)



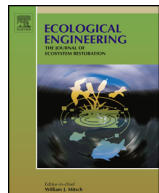
Steven Cooke
Carleton University
683 PUBLICATIONS 13,203 CITATIONS

[SEE PROFILE](#)



C. Katopodis
130 PUBLICATIONS 1,911 CITATIONS

[SEE PROFILE](#)



The hydraulics of a vertical slot fishway: A case study on the multi-species Vianney-Legendre fishway in Quebec, Canada



Bryan A. Marriner^a, Abul B.M. Baki^a, David Z. Zhu^{a,*}, Steven J. Cooke^b, Christos Katopodis^c

^a Department of Civil and Environmental Engineering, University of Alberta, Edmonton, Alberta T6G 2W2, Canada

^b Fish Ecology and Conservation Physiology Laboratory, Department of Biology and Institute of Environmental Science, Carleton University, 1125 Colonel By Drive, Ottawa, Ontario K1S 5B6, Canada

^c Katopodis Ecohydraulics Ltd., 122 Valence Avenue, Winnipeg, Manitoba R3T 3W7, Canada

ARTICLE INFO

Article history:

Received 26 January 2015

Received in revised form

14 November 2015

Accepted 26 January 2016

Keywords:

Computational fluid dynamics

Field measurements

Flow velocity

Multi-species passing fishway

Vertical slot fishway

Water level

ABSTRACT

This paper presents an overall assessment of the hydraulics of a vertical slot fishway, the Vianney-Legendre vertical slot fishway on the Richelieu River in Quebec, Canada, which has been shown to be successful for passing a variety of fish species, including lake sturgeon. The fishway has a number of features that combine for a unique design. This includes two turning pools, shorter and narrower than recommended regular pools, and a low overall gradient. Detailed field measurements of the water levels and velocity patterns were obtained and a computational fluid dynamics modeling study was conducted. The model study evaluates the performance of various regular pool geometries based on fishway hydrodynamics. Low overall fishway gradient was shown to result in a fishway hydraulically suitable to fish passage, overcoming non-optimal pool dimensions. The relationship between discharge and corresponding average water depth in the pools, under both uniform and non-uniform flow conditions, using the discharge coefficient enabled us to simulate the distribution of water levels in a vertical slot fishway. Two distinct flow patterns were observed in a regular pool depending on the shape ratios between the pool's length and width. This study also assessed the spatial variation of velocity magnitude in the vertical plane to reveal regions of upwelling, downwelling, and the formation of eddies and dead flow zones that have potential importance for fish migration.

© 2016 Elsevier B.V. All rights reserved.

1. Introduction

Fishways are built all over the world to restore connectivity where rivers have been disconnected by hydraulic barriers of natural or man-made origin such as hydro-electricity producing facilities, flood control structures, and natural water falls (Clay, 1961). A fishway's primary function is to provide passage over hydraulic barriers to fish swimming upstream. A number of fishway designs are commonly used across the globe and are placed under two broad categories: engineered structures, and nature-like fishways. Engineered structures are built with "hard" construction materials (e.g., steel, reinforced concrete) and include the pool and weir, Denil, and vertical slot designs. Nature-like fishways are constructed using natural, or so-called "soft" materials (e.g., boulders,

gravel, and logs) and are designed to mimic the hydraulic, bed, and bank conditions of a natural stream (Baki et al., 2014a, 2014b; Katopodis et al., 2001).

The vertical slot fishway, hereinafter referred to as VSF, is an engineered structure. Variations of this design are commonly used around the world. For example, Canada has 37 documented VSFs, making it the second most common design in the country (Hatrty et al., 2013). They are made up of one or more sloping linear rectangular channels separated into pools, commonly known as regular pools, via transverse baffle walls. The baffle wall openings are the full height of the water column allowing flow to travel downstream from pool to pool (Rajaratnam et al., 1992b). VSFs are suitable for use in a large range of hydraulic and biologic environments and have several advantages over other designs (Katopodis and Williams, 2012). They are often the design of choice where a relatively large fishway is required. The baffle wall opening enables fish to ascend the fishway at their preferred swimming depth, accommodating species that cannot or will not jump to pass between pools. This is advantageous over 'overflow' designs (e.g., pool and

* Corresponding author.

E-mail addresses: david.zhu@ualberta.ca (D.Z. Zhu), KatopodisEcohydraulics@live.ca (C. Katopodis).

weir) which require fish to jump out of the water to ascend pools (Warren and Beckman, 1993). Each regular pool in a VSF has an area of low velocity for fish to rest during upstream passage (Rajaratnam et al., 1992b). Another important feature of the VSF is that it operates through a range of upstream and downstream river level conditions. This makes them suitable to sites where fish passage is needed at different times of the year to accommodate the migrations and movements of a community of fish species, as well as to mitigate the effects of varying water levels from year to year.

As the use of fishways changes from passing a target species to encompassing passage for whole fish communities, interest in fishway designs that are able to pass multiple species has increased (Thiem et al., 2013). Thiem et al. (2013) documented the successful upstream passage of 18 species of fish, and Desrochers (2009) indicated that annually over 35 species pass the Vianney-Legendre fishway, hereinafter called the “site fishway”, and the focus of this study. Members of the salmon (*Salmonidae*), sturgeon (*Acipenseridae*), perch (*Percidae*), sucker (*Catostomidae*), sunfish (*Centrarchidae*) and catfish (*Ictaluridae*) families, among others, all passed through the site fishway, demonstrating its ability to serve a diversity of fish. Included in this list of species are copper redhorse *Moxostoma hubbsi* and lake sturgeon *Acipenser fulvescens*. The Committee on the Status of Endangered Wildlife in Canada (COSEWIC) listed copper redhorse as ‘endangered’. Copper redhorse are endemic to Quebec and are known to live in just three river systems. COSEWIC has categorized lake sturgeon populations throughout Canada as ‘threatened’, ‘endangered’ or of ‘special concern’ (COSEWIC (1) and (2), 2012). The site fishway is one of few worldwide to have documentation of successful passage of a species of sturgeon (Thiem et al., 2011).

There have been a number of experimental and numerical studies (e.g., Rajaratnam et al., 1992b; Wu et al., 1999; Liu et al., 2006; Cea et al., 2007; Wang et al., 2010; Puertas et al., 2012; Bombac et al., 2014; Perez et al., 2014) addressing the flow characteristics in several designs of VSFs. They have focused on water surface profiles, depth-discharge relationships, velocities, turbulent kinetic energy, and energy dissipation rates within regular pools. There are few documented field studies providing general observations, and field measured data are limited. Accordingly, a need existed to study the entire fishway (considering regular and turning pools) to gain an understanding of its overall hydraulics as a system and to complete this study in a field setting. As a result this study focused on the overall hydraulics and design of the site fishway which was selected for case study because it is known to pass a diversity of species and has unique design features.

The site fishway has shorter and narrower regular pools lengths and widths as compared to the recommended dimensions of Rajaratnam et al. (1992b). It is formed of three straight segments of regular pools connected via two turning pools, which produces a compact and efficient design with the fish entrance located close to the hydraulic barrier. The overall slope of the fishway is also very mild in comparison to design limits for vertical slot fishways (Bell, 1973; Larinier et al., 1999; Marriner et al., 2014; Rajaratnam et al., 1992b).

The goal of this study was to understand the hydraulics of the site fishway. Here we used water level, velocity, and flow measurements taken in the field to understand the site fishway's flow type, allowing the water surface profile to be predicted. The flow characteristics in both regular and turning pools were investigated in the field. Vertical velocity profiles were measured in the field providing an understanding of velocities through the height of the water column. A detailed account of the study site and fishway were completed, and an overall assessment of the site fishway's hydraulics was generated. Moreover, a computational fluid dynamics (CFD) model study was used to examine the flow hydrodynamics to evaluate the performance of various regular pool geometries. Here, five

regular pool geometric scenarios were modeled to assess the effect of changing length and/or width on the pool's hydrodynamics. The first scenario used the site fishway's dimensions and had the smallest lengths and widths. In the remaining four scenarios length and width were increased incrementally until the accepted dimensions recommended for design were reached in the fifth scenario.

It is expected that this study along with a concurrent hydraulics study evaluating the characteristics of turning pools will be used with field-based biological studies of fish passage and behavior at the site fishway to provide engineers and biologists with tools to evaluate the site fishway's performance in terms of hydraulics and fish passage (Marriner et al., 2014; Thiem et al., 2011; Thiem et al., 2013).

2. Field study and numerical modeling

The Richelieu River flows north from its headwaters of Lake Champlain, situated along the state borders of New York and Vermont in USA, to Sorel-Tracey in southwestern Quebec, Canada. The site fishway is on the Richelieu River 18 km upstream of the confluence with the St. Lawrence River and is situated just outside of Saint-Ours, Quebec. The fishway is on the west bank of the river adjacent to the 180 m wide and 3.4 m high Saint Ours Dam. For the period of 1938–2012 the Richelieu River's average maximum daily, average minimum daily, and mean discharges were approximately 800 m³/s, 175 m³/s and 360 m³/s, respectively (Wateroffice Canada, 2015).

Built in 2001–2002, the site fishway is a vertical slot design constructed of reinforced concrete, with steel baffle walls. The site fishway (Fig. 1) has 18 pools in total; 12 regular pools, 2 turning pools, entrance and exit pools, and 2 pools immediately downstream of the entrance pool with slot openings in their centre. Three segments of linearly regular pools are connected via 180° turning pools (pools 8 and 13) at the segment ends.

Upstream river water enters the fishway through the entrance pool, flows through pools 1–7, turns 180° in pool 8, flows through pools 9–12, turns 180° in pool 13, flows through pools 14–16 and then enters the river downstream of the dam through the exit pool. The fishway has a linear length of 48.5 m and width of 9.60 m. Regular pools (i.e., pools 3, 4, 5, 6, 7, 9, 10, 11, 12, 14, 15, 16) are 3.50 m long, l , and 3.00 m wide, b , see Fig. 2a. Turning pools (i.e., pools 8 and 13) are 6.30 m wide, b_t . The back wall is semi-circular with a radius, R , of 3.15 m. Pool 13 has a maximum length, l_t , of 3.50 m from centre wall to back wall, see Fig. 2b, while pool 8 is shorter with $l_t = 3.35$ m.

The fishway floor elevations at the upstream entrance and downstream exit are 4.85 and 2.30 meters above sea level (m.a.s.l.), respectively, resulting in a 2.55 m elevation change. Table 1 summarizes the pool floor elevations. Regular pools floors are sloping; each pool has a 0.075 m elevation drop between the upstream and downstream ends. In addition, Pools 3–16 have a 0.075 m elevation change between pools across the slot area. The sum of these elevation changes produces a 3.95% slope for pools 3–16.

The upstream entrance pool has a 0.85 m wide gate. Pool 1 has 1.00 m and 1.20 m wide slots in the center of its upstream and downstream baffle walls, respectively. Slots from the downstream end in pool 2 through to the downstream end in pool 16 shared a common design. The slot width, b_0 , is 0.609 m, the long baffle is 2.12 m long, attached to its end is a 1.0 m × 0.5 m guide extending upstream. The short baffle is 0.46 m long. The slot opening is at a 57° angle to the longitudinal flow direction. The downstream exit pool has a 3.50 m wide gate. The length and width to slot width ratios in the site fishway's regular pools are $l = 5.75b_0$ and $b = 4.9b_0$. These are less than $l = 10b_0$ and $b = 8b_0$, established across North America and Europe as the recommended design dimensions for regular

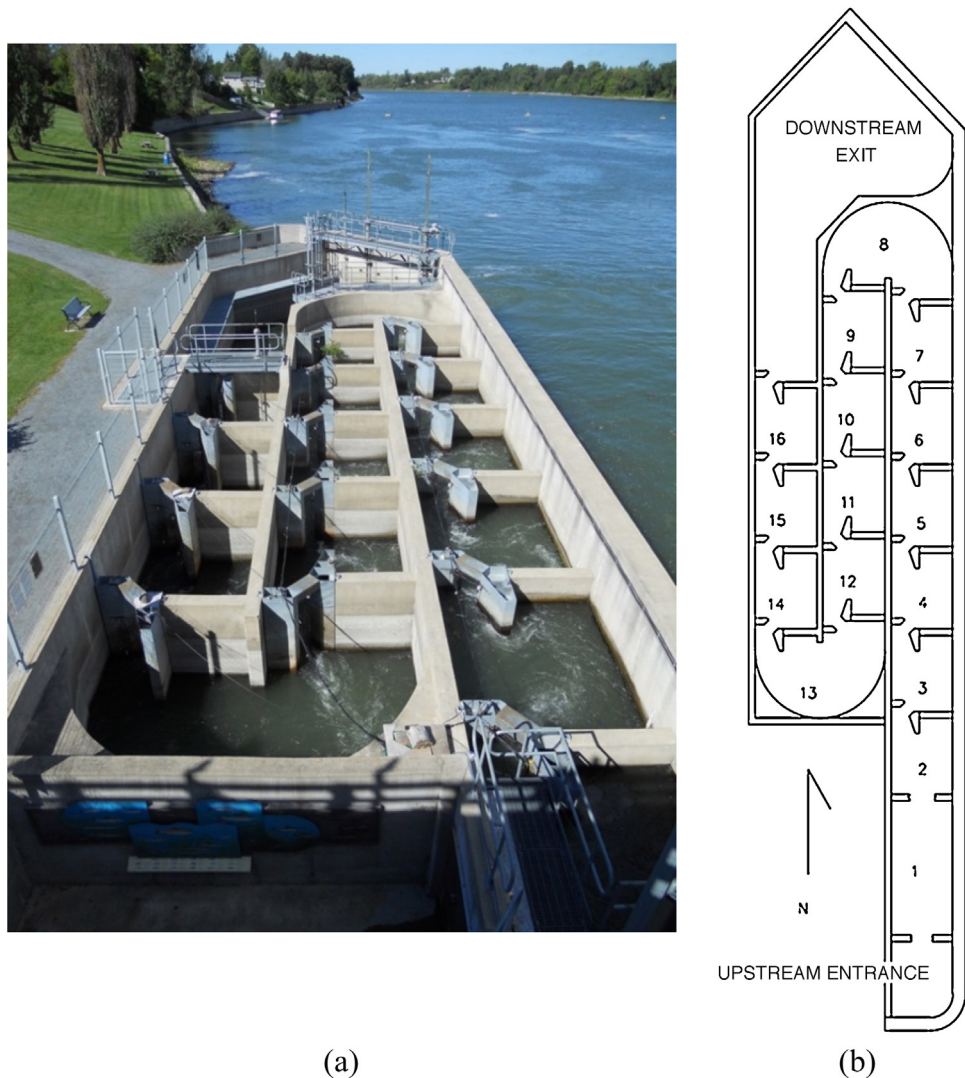


Fig. 1. The Vianney-Legendre vertical slot fishway (a) fishway and the adjacent west bank of the river with a downstream (north) orientation, (b) plan view diagram.

Table 1

Vianney-Legendre vertical slot fishway pool floor elevations, as measured in metres above sea level (m.a.s.l.).

Pool no.	Pool floor elevation	
	Upstream end (m.a.s.l.)	Downstream end (m.a.s.l.)
Entrance	4.85	–
1	4.85	4.795
2	4.70	4.625
3	4.55	4.475
4	4.40	4.325
5	4.25	4.175
6	4.10	4.025
7	3.95	3.875
8	3.80	3.725
9	3.65	3.575
10	3.5	3.425
11	3.35	3.275
12	3.20	3.125
13	3.05	2.975
14	2.90	2.825
15	2.75	2.675
16	2.60	2.525
Exit	2.45	2.30

pools ([Clay, 1961](#); [Bell, 1973](#); [Larinier et al., 1999](#); [Rajaratnam et al., 1992b](#)). Generally, it is accepted that the length and width of pools can vary from 7 to 12 and from 5 to 9 times the slot width, respectively ([Wang et al., 2010](#)).

Field measurements were gathered from July 18–29, 2011 and from June 4–8, 2012. The Schlumberger Water Services Mini-Diver pressure and temperature dataloggers were used to record continuous water levels in the fishway pools. The manufacturer stated an accuracy of ± 0.005 m H₂O, with a resolution of 0.002 m H₂O ([Schlumberger Water Services, 2011](#)). In 2011 dataloggers were deployed from July 18–29 in pools 5, 8, 11, 13, and 15, at a measurement frequency of 1 min. In 2012 dataloggers were deployed from June 5–July 30 in pools 1, 6, 7, 8, 9, 12, 13, 14 and 15; at a measurement frequency of 4 min. [Parks Canada \(2010\)](#) provided water levels immediately upstream and downstream of the St. Ours Dam. Water depths in Pools 3–16 were measured using a staff gauge on July 22, 2011 from 5 to 5:30 pm EST.

Instantaneous point velocity measurements were recorded with a Nortek Vectrino Acoustic Doppler Velocimeter (ADV) ([Nortek AS, 2011](#)). Measurements were taken in pools 5, 8, 13 and 15. A grid spacing of 0.50 m \times 0.50 m was used for measurements, with increased point densities in the slot and jet flow areas. All points

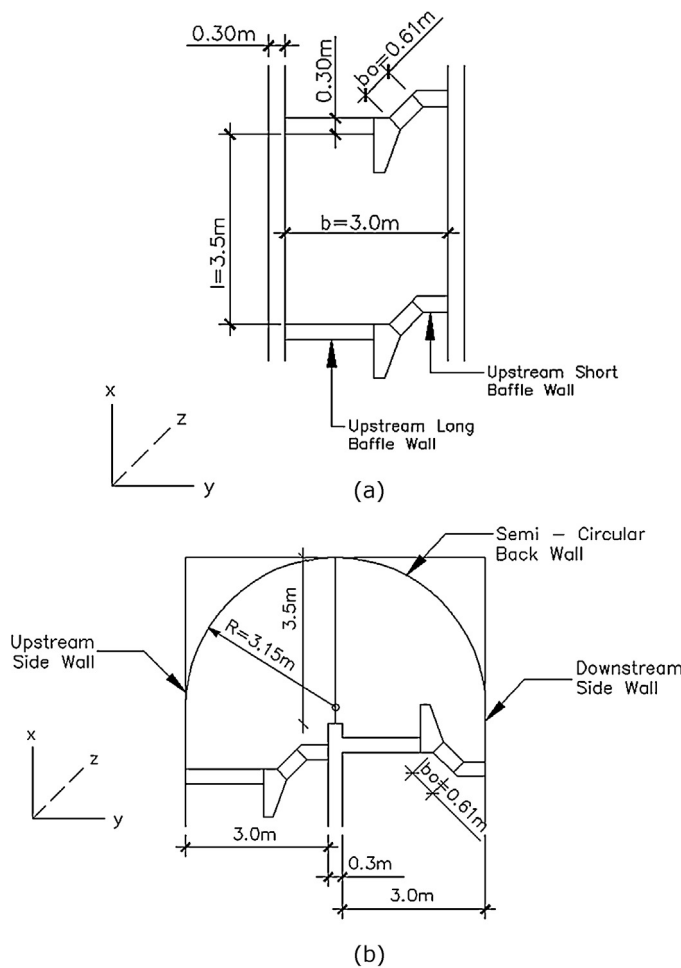


Fig. 2. Plan view schematic diagrams of (a) a regular pool and (b) turning Pool 13 in the Vianney-Legendre fishway.

were recorded at a fixed elevation 0.50 m below the water surface. Attempts were made to also record points 1.50 m below the water surface; however, the ADV produced low quality data due to large vibrations in the setup. The manufacturer specified velocity data collected with the ADV to be accurate to $\pm 0.5\%$ of the measured value, with a maximum accuracy of $\pm 0.001 \text{ m/s}$ (Nortek AS, 2011). This study's maximum recorded velocity was 1.40 m/s, theoretically accurate to $\pm 0.01 \text{ m/s}$. Prior to data collection preliminary testing was done to determine the required ADV sampling period for accurate time-averaged velocity measurements. Sample test periods of 30–120 s were taken, and velocity became nearly constant after 45 s. All point measurements were recorded for 180 s at a sampling frequency of 25 Hz. Measurements were taken in the x , y , z coordinate system, which correspond to u , v , and w velocities averaged over the sampling period to produce time averaged velocities. The data correlation ranged between 42.5% and 94.5% in the time-averaged velocity measurements. All points had a correlation value above 40% which is the minimum accepted correlation for time-average velocity and therefore were deemed accurate.

Vertical velocity profiles within the fishway were measured using a Sontek 3.0 MHz acoustic Doppler profiler (ADP). Profiles were recorded 0.61 m downstream of, and perpendicular to, the slot as flow entered pools 4, 5, 8, 13, 14, 15 and 16, where bin size = 0.15 m and blanking distance = 0.2 m. The ADP measures the velocity profile over the full height of the water column. Simultaneous to recording velocities, the ADP recorded water depth in pools 3–16.

Table 2

Summary of the regular pool geometry scenarios simulated using computational fluid dynamics modeling.

Scenario	Length, l (m)	Width, b (m)	Slot width, b_0 (m)	$l:b_0$	$b:b_0$	Slope (%)
1	3.5	3	0.609	5.75	4.9	3.95
2	4.87	3	0.609	8	4.9	3.95
3	6.09	3	0.609	10	4.9	3.95
4	4.87	4.87	0.609	8	8	3.95
5	6.09	4.87	0.609	10	8	3.95

A commercial CFD solver (ANSYS CFX) was used to create a numerical model simulating regular pools 3–7. The model uses the finite volume method to solve the three-dimensional Navier–Stokes equation using the standard $k-\varepsilon$ turbulence model. The model was previously validated in a study focusing on the hydraulics in the site fishway's turning pool 13. A complete outline of the model, model development, and corresponding boundary conditions used is provided in Marriner et al. (2014).

As the site fishway's regular pool dimensions are shorter and narrower than recommended, this CFD model study was undertaken to assess how the smaller pool dimensions affected the fishway hydrodynamics and jet velocity decay in comparison with longer and wider dimensions. Five geometric scenarios were compared; their dimensions are summarized in Table 2. Two widths $b = 4.9b_0$, $8b_0$ and three lengths $l = 5.75b_0$, $8b_0$, $10b_0$ were tested. Scenario 1 represented the site fishway $l = 5.75b_0$, $b = 4.9b_0$. Scenarios 2, 3, and 4 were incrementally wider and/or longer than Scenario 1; and Scenario 5 had the recommended design dimensions $l = 10b_0$, $b = 8b_0$. By increasing l and b dimensions independently from the site fishway's dimensions (Scenario 1) to the recommended dimensions (Scenario 5), each variable's effect on flow structure and jet velocity decay were shown. This is important to designers because it allows them to understand the significance of dimensions and can help them to make more informed decisions when assessing existing or constructing new fishways.

3. Results and discussion

3.1. Water surface profiles

Water levels in the Richelieu River typically peak in late April to early May during spring freshet. Upstream of the dam water levels fluctuate naturally until they drop to 6.85 m.a.s.l. This typically occurs in June or July, after which water levels are maintained at 6.85 m.a.s.l. ± 0.1 m during the summer months to support recreational boater traffic. Downstream of the dam water levels decrease naturally until September when they reach their annual minimum. During the spring and summer of 2011 abnormally high water levels were present throughout the Richelieu River system. Water levels in 2012 were less extreme and closer to historical averages (MDDEP (1) and (2), 2013).

In the spring during freshet high water levels can flood the entire site fishway. In less severe cases a portion of the downstream end of the fishway may be submerged. Under high water levels, the site fishway is typically submerged such that when the dam gates are opened there is a negligible difference in water levels between the upstream and downstream sides. Under these conditions the fishway is non-operational; fish can simply swim past the lowered dam barriers and continue on upstream unimpeded.

Due to the great influence of tailwater river levels, the water surface profiles in a vertical slot fishway can be uniform, where the depth, h , of water in each pool is approximately the same; or non-uniform, with a backwater profile (M1 curve) or a drawdown profile (M2 curve) (Chow, 1959; Rajaratnam et al., 1986). Fishways are designed to run at uniform flow condition as this will require

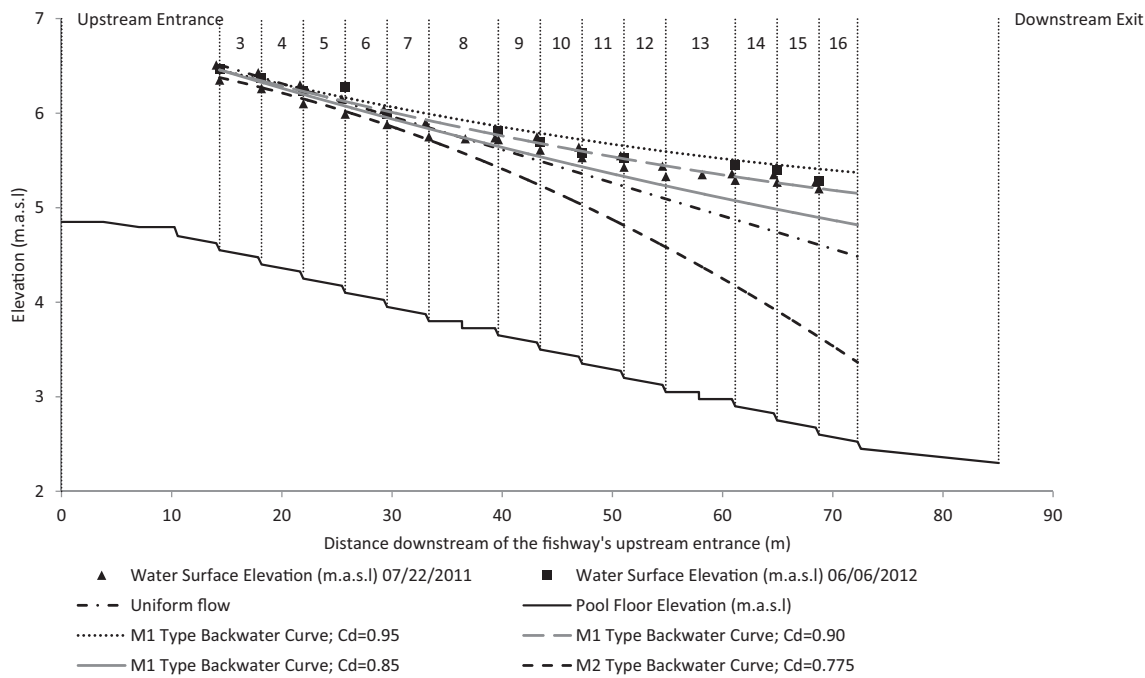


Fig. 3. Water surface elevations for Pools 3–16 of the Vianney-Legendre fishway. Note: The upstream ends of Pools 3–16 are indicated by dashed lines.

the minimum fishway length by having an equal water level drop in each pool. When the tailwater level rises above the uniform condition, the water level drop between pools, Δh , close to the downstream end of the fishway decreases. The backwater condition may diminish fish attraction to the fishway entrance due to lower flow velocities from decreased Δh values. On the other hand, when the tailwater level drops below the uniform flow level (drawdown profile or M2 curve), Δh increases towards the downstream end of the fishway. The drawdown condition is not desired given the potential of excessive flow velocity created by a larger Δh .

With an M1 curve, the slope of the water surface profile inside the fishway is less than the fishway pool floor slope, whereas it is greater with an M2 curve. Under uniform flow conditions the values of h and Δh are constant through all pools, and the water

surface and pool floor slopes are equal. The water surface profiles of M1 type backwater curves, uniform flow conditions, M2 type drawdown curves, and measured water surface profiles on July 22, 2011 and June 6, 2012 plotted against the site fishway's pool floor elevations are shown in Fig. 3.

In both data sets (July 22, 2011 and June 6, 2012) flow was found to be non-uniform with an M1 type backwater curve, as shown in Fig. 4. The water surface profile approached uniform flow conditions at the upstream end of the fishway, from the entrance to pool 8. Here the flow was less affected by the high tailwater levels in the river downstream of the fishway, resulting in a slower rate of increase to h in this section. After the transition in pool 8 the water surface profile was more strongly affected by tailwater levels and h increased more rapidly. The M1 backwater curve in

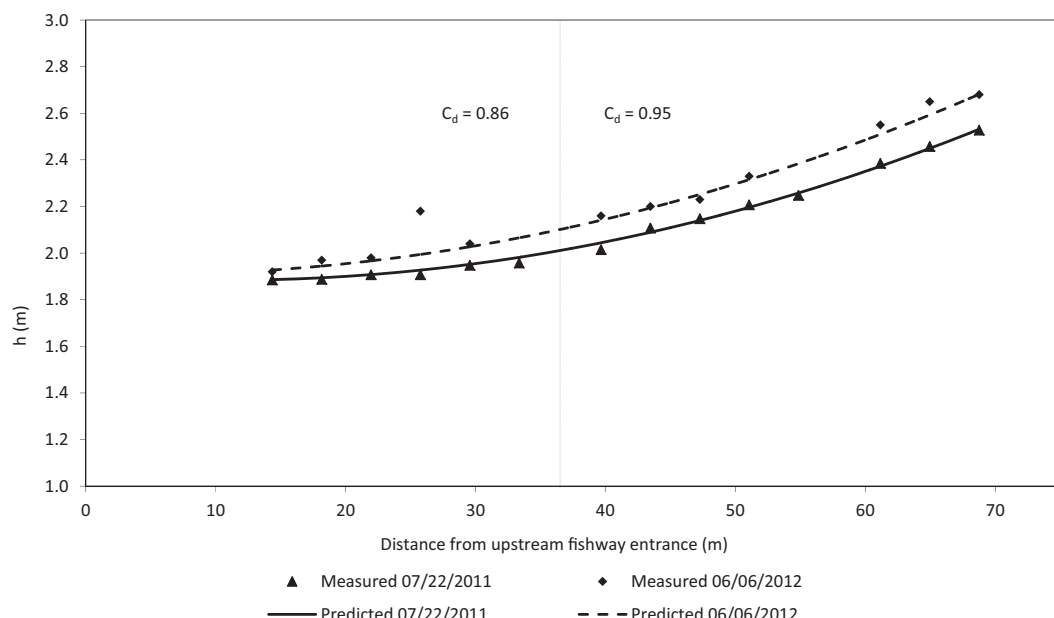


Fig. 4. Measured vs predicted water surface profiles at the Vianney-Legendre fishway.

both data sets showed the effect the river's tailwater levels had on the site fishway's water surface profile. The flow into the upstream entrance was constant with the upstream water levels maintained at 6.85 ± 0.1 m.a.s.l., therefore the natural fluctuation of the tailwater levels was the controlling factor of the water surface profile through the site fishway. In the spring and early summer, when tailwater levels are high, there will be an M1 backwater curve. It is noted that the fishway behaves as a mild sloping channel. The high rate of energy dissipation in the pools enables the fishway to behave as a mild sloping channel even though it has a steep slope.

A fishway design needs to take into consideration the water surface profile because it will vary throughout the year depending on river discharge. Traditionally, fishways were designed to pass salmon whose upstream migrations are concentrated over shorter periods of time each year. Now as fishway design evolves to encompass fish communities, there are more variables to be accounted for in the design of a fishway. For example, having a uniform water surface profile may be targeted in the middle of the annual period of use, to allow for passage to occur for as long as possible on either side of the middle of the desired passage period. In this way a fishway can accommodate a wide range in natural variables into its operation. These natural variables include: fluctuating river conditions from year to year, whether the river is a controlled or uncontrolled system, variability in migration times within a species, duration of species migrations, various migration periods of design target species, and desired annual duration of fishway operation. Each fishway will have its own unique set of natural variables. Further study is required to assess the site fishway's annual operational duration and associated patterns of fish passage over this period of time.

3.2. Water depth and discharge relationship

For the site fishway, the relationship between the discharge and corresponding average pool water depth was investigated. This relationship is essential when dimensioning a VSF. The flow rate, Q , through a vertical slot can be predicted following the equation proposed by [Clay \(1961\)](#):

$$Q = C_d \sqrt{2g\Delta h} * (b_0 h) \quad (1)$$

where C_d is a discharge coefficient, b_0 is the slot width, h is the flow depth at the upstream side of the slot, and Δh is the change in water level across the slot. In Eq. (1) $C_d \sqrt{2g\Delta h}$ and $b_0 h$ represent the flow velocity and flow area components, respectively, of Q . [Rajaratnam et al. \(1992a\)](#) in their laboratory experiments predicted values of $C_d = 0.3–1.3$ for a variety of vertical slot designs tested. They measured $C_d = 0.6–0.8$ for a Design 1 type regular pool; the baffle geometry in Design 1 closely resembles the design of the site fishway's baffles.

Eq. (1) was used to determine C_d for the site fishway. Using a known $Q = 1.63 \text{ m}^3/\text{s}$ from measurements taken in July 2011, and a known h measured in slot 3, an iterative solver was used to calculate h in slots 3–16, where the slot number represents the pool the flow is entering. Predicted h values were then compared to h values measured in the field on July 7, 2011 and June 6, 2012. The solver was repeated increasing or decreasing C_d until there was strong agreement between the predicted and measured data sets. On July 7, 2011 h values were recorded at the centre of the downstream long baffle wall in the pool upstream of the slot, and h measurements on June 6, 2012 were recorded 0.61 m downstream of the slot center. In both cases h measured was assumed to be approximately equal to h in the slot and therefore acceptable for comparison to h predicted in Eq. (1).

The comparison of h predicted against h measured on July 7, 2011 and June 6, 2012, respectively, is shown in Fig. 4. Here the

two different flow sections are shown. From the entrance of the fishway downstream to pool 8 $C_d = 0.86$, and from pool 8 to pool 16 $C_d = 0.95$. In pool 8, which is the upstream turning pool, a transition in the flow occurs. There was strong agreement between predicted and measured h values, with the mean absolute error (MAE) equal to 0.01 m on July 7, 2011 and 0.04 m on June 6, 2012.

The discharge coefficient (C_d) is a function of various parameters including: pool geometry, flow depth, flow rate, and velocity. At the site fishway C_d was greater than the 0.6–0.8 calculated by [Rajaratnam et al. \(1986\)](#) in a Design 1 regular pool. This was because less jet velocity decay occurred through the shorter and narrower regular pools in the site fishway (discussed later). Less decay led to larger residual velocities traveling through the pool, resulting in greater jet velocities and a correspondingly larger C_d (in comparison to a Design 1 regular pool). Also, C_d values at the site fishway were significantly greater than 0.65–0.75, generally adopted when designing vertical slot fishways in France ([Wang et al., 2010](#)).

3.3. Flow patterns and velocity

The velocity field diagrams in the x, y -plane at 0.5 m below the water surface for pools 5 and 15, are shown in Fig. 5. It is important to note that due to field constraints, point velocities were measured following a coarse grid and measurements were not taken close to the pool walls. Jet flow entered the pool through the upstream slot, traveling downstream in the direction of the opposite corner (at the intersection of the downstream long baffle and longitudinal walls). As the jet flow approached the pool's center it turned, curving in the direction of the slot, and flowed downstream out of the pool through the slot. The jet energy was dissipated as the jet flowed through the pool. Two resting areas were generated in the pool, one on either side of the jet flow. They are characterized by low velocities and flow recirculation, provide resting spaces for fishes ascending the ladder ([Wang et al., 2010](#)).

Previously, different studies (e.g., [Wu et al., 1999](#); [Liu et al., 2006](#); [Wang et al., 2010](#)) have concluded that there are two typical flow patterns in a regular pool depending on the pool's slope and width, referred to as FP1 and FP2. In FP1, the principal flow leaving the slot enters the pools as a curved jet which disperses into the pool center before converging again towards the next slot, and in FP2, the jet has a curved form and hits the opposite side wall. The flow pattern in pools 5 and 15 was similar to flow pattern FP1, where a jet from the slot that traversed the pool with decreasing velocity and two recirculation zones were generated, one on either side of the jet (although the large recirculation zone was not very clear-cut due to lack of detailed measurement points, as mentioned above). [Wang et al. \(2010\)](#) also found the flow pattern to be similar to FP1 for $b/b_0 < 7$ and at a low slope (5%).

In contrast with regular pools, flow patterns in the turning pools saw jet streamlines flowing around a large circular concentric recirculation area in the pool center. Due to the asymmetric geometry the jet did not enter through the pool's center and there were flow recirculation eddies sitting on either side of the jet ([Marriner et al., 2014](#)). A detailed analysis of the site fishway's turning pool hydraulics can be seen in [Marriner et al. \(2014\)](#).

A detailed study of hydrodynamics in regular pools was completed using a numerical model. The numerical study examined the flow patterns of five different geometric ratios for l/b_0 varying from 5.75 to 10 and b/b_0 varying from 4.9 to 8 at a 3.95% slope. [Wang et al. \(2010\)](#) observed the flow patterns for length $l = 10b_0$ and widths ranging from $b = 5.7b_0$ to $9.0b_0$. Earlier studies focused on length and width ratios of $l = 10b_0$ and $b = 8b_0$, respectively. Studying a range of lengths and widths enabled us to identify the changes in flow patterns due to varying both pool length and width.

The velocity distributions in the horizontal plane parallel to the floor at depth of $z = 0.5h$ for the five scenarios simulated using

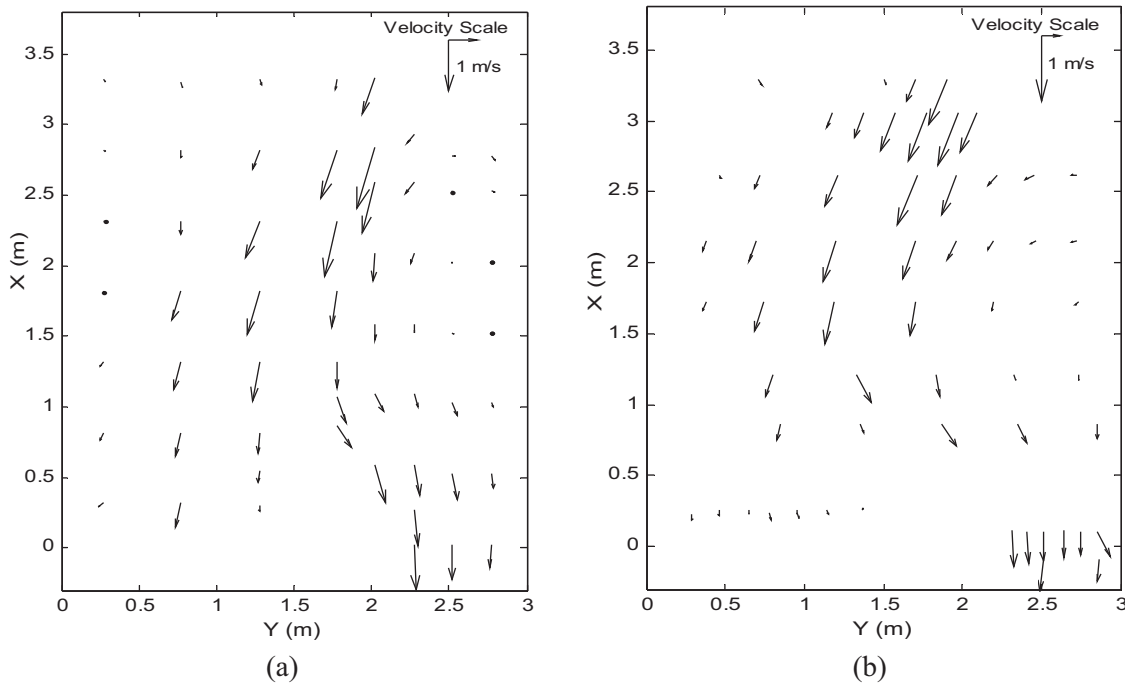


Fig. 5. Time-averaged velocity field in the x - y plane 0.50 m below the water surface in the Vianney-Legendre fishway (a) Pool 5, and (b) Pool 15.

CFD modeling are shown in Fig. 6. The results confirmed that the flow pattern in Scenarios 1 and 4 was similar to flow pattern FP1, whereas in Scenarios 2, 3, and 5 it was similar to pattern FP2. At a slope of 5%, Wang et al. (2010) found the transition between FP1 and FP2 takes place when b/b_0 was very close to 7.0. Therefore, following this observation by Wang et al. (2010), the flow patterns in Scenarios 2–3 and Scenario 4 are in disagreement with these results. Depending on the regular pool length and width ratio (l/b), the present results demonstrated two distinct flow patterns (FP1 and FP2), occurred for $l/b < 1.1$ and $l/b > 1.3$, respectively, and an apparent transition between FP1 and FP2 takes place for a l/b ratio of about 1.2. Therefore, it is concluded that the flow in a regular pool is influenced by the length to width ratio (l/b). It is recommended that future physical and numerical model studies are undertaken to investigate different shape ratios, l/b , to confirm the transition between FP1 and FP2.

To understand the behavior of the jet flow formed at the slot, numerical results were used following the jet trajectory. Fig. 7 shows the transverse distributions of the mean jet velocity, U_j , in the x_j direction for Scenario 1, where U_j is the time-averaged longitudinal jet velocity and x_j is the distance along the curved jet center line from the entrance slot. The flow was similar to the Gaussian distribution of a plane turbulent jet (Rajaratnam, 1976). However, the structure was not symmetric about the x_j axis because the jet does not enter through the pool's center and there were flow recirculation regions on either side of the jet. The velocity U_j is made dimensionless by dividing it by U_{sm} , where U_{sm} is the maximum time-averaged slot velocity in the x_j direction.

The dissipation of jet velocity was evaluated for Scenarios 1–5 and is shown in Fig. 8. The normalized maximum jet velocity U_{jm}/U_{sm} is plotted against $x_j/0.5b_0$, where U_{jm} represents the maximum jet velocity at a distance x_j from the entrance slot. Corresponding curves are plotted for a plane turbulent jet and the mean curve from a previous study of a Design 18 (Liu et al., 2006; Rajaratnam et al., 1992b) regular pool. Measurements are taken starting at $x_j/0.5b_0 = 0.7$. Scenarios 1 and 5 had the shortest and longest length of jet ($x_j/0.5b_0 = 8.7$ and 18.1) and the corresponding

value of normalized jet velocity (U_{jm}/U_{sm}) was about 0.7 and 0.3, respectively. The length of jet was 0.48 times shorter and the corresponding normalized jet velocity was about 2.1 times larger in Scenario 1 as compared to Scenario 5. The jet velocity decay in all scenarios was similar to that found by Liu et al. (2006):

$$\frac{U_{jm}}{U_{sm}} = 1 - 0.035 \frac{x_j}{0.5b_0} \quad r^2 = 0.77 \quad (2)$$

At a distance of $x_j/0.5b_0 = 12$, the ratio U_{jm}/U_{sm} for the jet travelling in the pool was around 0.4–0.6 in all scenarios. These values lie between the values found by Wu et al. (1999), Wang et al. (2010), and Liu et al. (2006), respectively 0.4, 0.4–0.5, and 0.5–0.6. It can be concluded that less jet velocity dissipation occurred in the shorter regular pool design used in the site fishway (Scenario 1) than the longer recommended design geometry (Scenario 5), which resulted in larger jet velocities through the pool. The jet velocity decay in all five scenarios was more rapid than in a plane turbulent jet. The rapid velocity decay is attributed to the flow entrainment and recirculation zones surrounding the jet flow caused by the longitudinal pool walls. Subsequently, the velocity decays faster in the turning pool as compared to a regular pool (Marriner et al., 2014). The more rapid decay in a turning pool is thought to be caused by the 180° turn required in the pool.

The field results show that U_{sm} in the core of the jet was very close to $U_{theor} = \sqrt{2g\Delta h}$. Wang et al. (2010) found that the maximum value of the velocity is reached in the jet at a distance from the slot slightly higher than the width of the slot. Using $U_{theor} = \sqrt{2g\Delta h}$ as a method of predicting maximum velocity in a vertical slot fishway has been previously used by Rajaratnam et al. (1986), Wu et al. (1999), and Liu et al. (2006) with good accuracy. Pools 5, 8, 13 and 15 had maximum measured velocity magnitude, U_{sm} , of 1.36 m/s, 1.40 m/s, 1.15 m/s and 1.00 m/s, respectively, see Table 3. The field ADV was used to measure U_{sm} in each of the 4 pools. Values of U_{sm} in pools 5 and 8 were greater than in pools 13 and 15 because Δh was higher in the upstream portion of the fishway than the downstream. In pools 5, 13, and 15 U_{sm} was compared to U_{theor} using

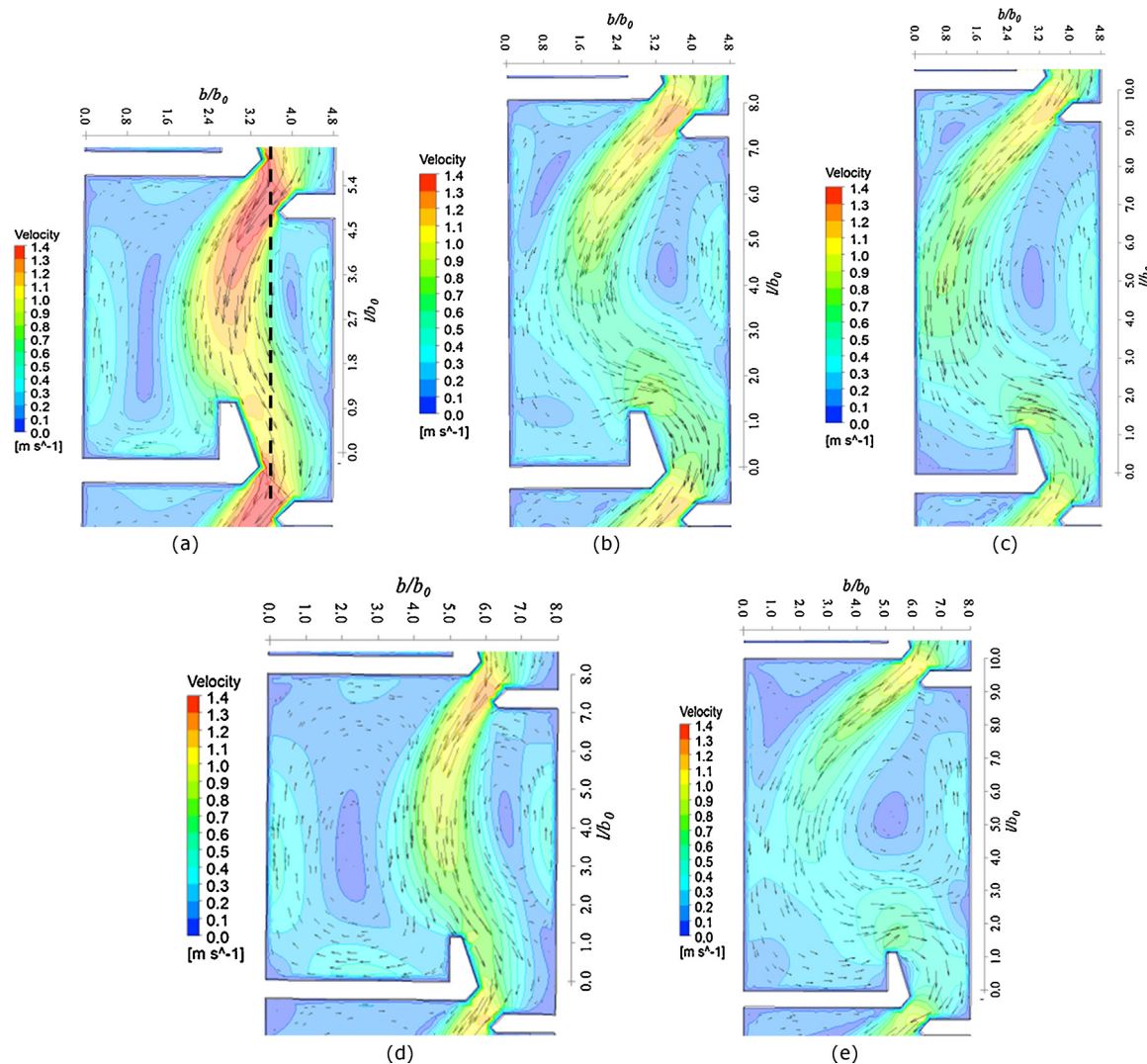


Fig. 6. Velocity distributions in regular pools at depths of $0.5 h$: (a) Scenario 1, $l = 3.5 \text{ m} \times b = 3.0 \text{ m}$; (b) Scenario 2, $l = 4.87 \text{ m} \times b = 3.0 \text{ m}$; (c) Scenario 3, $l = 6.09 \text{ m} \times b = 3.0 \text{ m}$; (d) Scenario 4, $l = 4.87 \text{ m} \times b = 4.87 \text{ m}$; (e) Scenario 5 $l = 6.09 \text{ m} \times b = 4.87 \text{ m}$. In (a) the dotted line is the fish passage path at depths of $0.5 h$ along which fish passage energetics are analyzed for the scenarios 1 through 5, $b_0 = 0.609 \text{ m}$.

Δh recorded at the time of U_{sm} measurement. U_{theor} was 28% greater than U_{sm} in pool 5, 16% greater in pool 13, and U_{theor} is equal to U_{sm} in pool 15, see Table 3. These results are consistent with other studies done on vertical slot fishways without turning pools which found

U_{sm} and U_{theor} to be nearly equal ([Liu et al., 2006](#); [Wu et al., 1999](#)). As well, the measured maximum velocity (U_{sm}) in the turning pool 13 was 1.15 m/s and calculated U_{theor} is 1.33 m/s, where U_{theor} is 16% greater than U_{sm} ([Marriner et al., 2014](#)). Therefore, these data

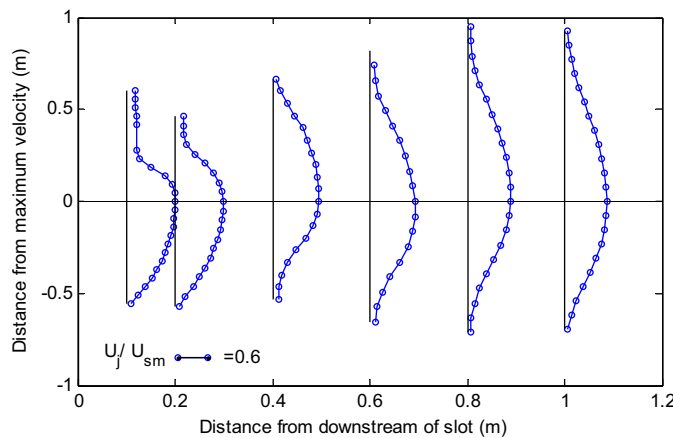


Fig. 7. Normalized distribution of longitudinal mean velocity in Scenario 1 jet flow.

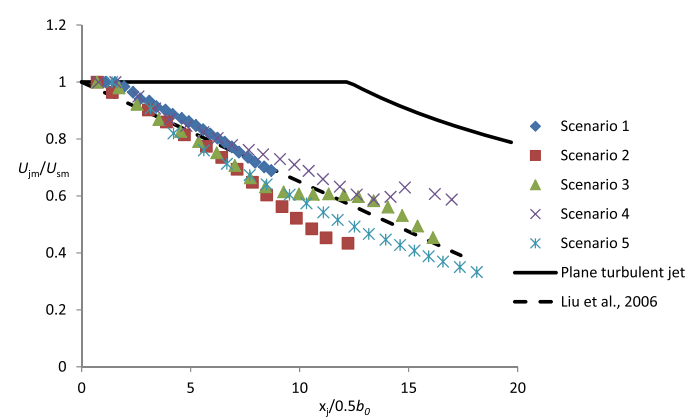


Fig. 8. Variation of normalized maximum velocity U_{jm}/U_{sm} with $x_j/0.5b_0$ for Scenarios 1–5.

Table 3

Velocity and flow rate field results recorded at the Vianney-Legendre fishway in July 2011.

Parameter	Pool 5	Pool 8	Pool 13	Pool 15
U_{sm} (m/s)	1.36	1.40	1.15	1.00
U_{theor} (m/s)	1.74	N/A	1.33	0.99
Q (m ³ /s)	1.54	1.79	1.62	1.57
h (m)*	1.89	2.09	2.34	2.58
b_0 (m)	0.609	0.609	0.609	0.609

Note: * h is presented at the time U_{sm} was recorded.

suggests U_{theor} can be used in vertical slot fishways with turning pools to estimate U_{sm} in both regular as well as turning pools.

Previously it was shown that high vertical velocity components are likely to influence the behavior of fish, particularly if velocities exceed the burst swimming capacity of fish (e.g., Peake et al., 1997). The maximum vertical velocity magnitude measured in field, W_m , was 0.29 m/s ($W_m = 0.23U_{sm}$) and 0.26 m/s ($W_m = 0.26U_{sm}$) in pools 5 and 15, respectively. In FP 2, Liu et al. (2006) found that the maximum vertical velocity can reach 20% of U_{sm} . The corresponding values in the turning pools 8 and 13 were 0.15 m/s and 0.14 m/s, respectively, less than 10% of U_{sm} in both pools (Marriner et al., 2014). The maximum upward positive velocities were downstream of the slot, after the jet entered the pool, and in the low velocity area adjacent to the longitudinal wall between the two short baffles. Maximum downward negative velocity was located upstream of the slot entrance. The mean vertical velocity, W , was 0.12 m/s and 0.091 m/s in pools 5 and 15, respectively. The time averaged vertical velocity, \bar{w} , was less than 0.1 U_{sm} in most areas of the pool; this allows fish to choose any preferred swimming depth (Liu et al., 2006), as long as velocities are sufficient to motivate upstream movements for the species and sizes migrating.

The detailed flow hydraulics or flow patterns in the horizontal plane parallel to the floor had previously been identified by different authors (Wu et al., 1999; Larinier et al., 1999; Liu et al., 2006; Wang et al., 2010). However, limited study examining flow pattern details in the vertical plane exists. The site fishway's velocity profiles and flow patterns in the vertical plane were investigated using field and numerical results.

The velocity profiles in regular pools 4, 5, 14, 15, and 16 measured using the ADP are shown in Fig. 9. Velocity is plotted against normalized flow depth, z/h , where z is the depth of flow

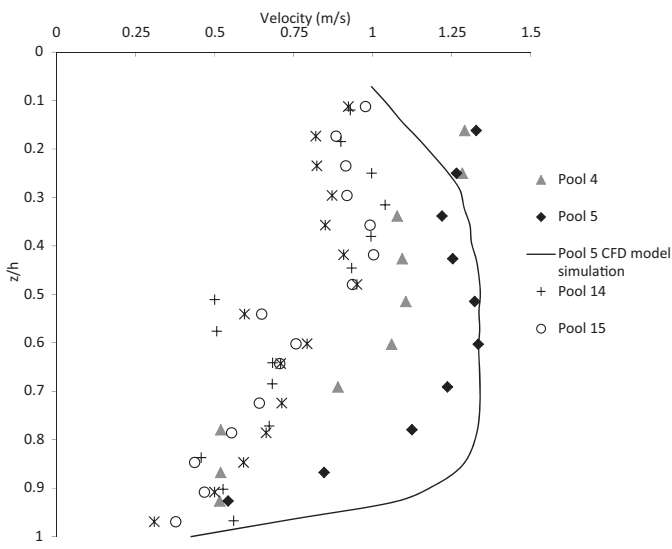


Fig. 9. Velocity profile 0.61 m downstream of the slot in Pools 4, 5, 14, 15 and 16 measured on June 6, 2012.

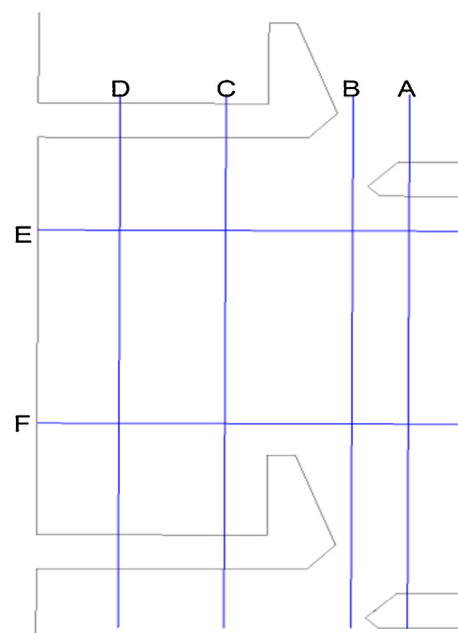


Fig. 10. The four longitudinal (A, B, C, and D) and two transverse (E and F) vertical cross sections are considered to examined the details flow patterns in Scenario 1.

beneath the water surface. Focusing on pools 5 and 15, velocity was fairly constant from the water surface to halfway down the water column ($z/h = 0.5$). Then at the approximate depth of $z/h = 0.5$ velocities began to decrease with increasing depth towards the pool floor. This decay in velocities towards the pool floor indicates that fish swimming close to the pool floor are exposed to slow velocities than fish higher up in the water column.

To assess the spatial variations of velocity magnitude in the vertical plane, six vertical cross sections were taken from the Scenario 1 numerical modeling results of pool 5 to show regions of upwelling and downwelling, as well as the formation of eddies and dead flow zones that have potential importance for fish migration. The location of the four longitudinal and two transverse vertical cross sections are shown in Fig. 10. Longitudinal cross sections (A, B, C, and D) show the two dimensional velocity in the x - z plane and the transverse cross sections (E, and F) show the two dimensional velocity in the y - z plane, see Fig. 11.

Longitudinal cross-section A is adjacent to the side wall between the two short baffle walls. In the upstream half of the pool, the velocities were relatively low (0.30 m/s) in the upstream direction. In the downstream half of the pool, flow changed direction, increasing with downstream pool distance, as it accelerated into the slot. In the center to downstream end of A, upwelling occurs, with water being supplied from the interior of the pool and downwelling occurs in the area adjacent to the upstream short baffle. B runs from the center of the upstream slot to the center of the downstream slot. At the upstream and downstream ends of this cross section are the entrance and exit slots, and the velocity magnitude was a maximum at these two locations. Away from the two slots, velocities decayed away from the upstream slot entrance, and then increased towards the downstream slot exit. Jet flow dominated and was in the downstream direction through the length of this section. Vertical velocity was minimal in this section. In C, velocity reached a maximum of 0.90 m/s in the center of the pool and decreased away from the center in the upstream and downstream directions, with a minimum magnitude of 0.30 m/s. Upwelling occurred adjacent to the upstream long baffle wall in the downstream direction and there was downwelling in the downstream direction between the tip of the slot baffle and the downstream long baffle wall. D had the lowest velocity magnitude (≤ 0.3 m/s), and the flow was in

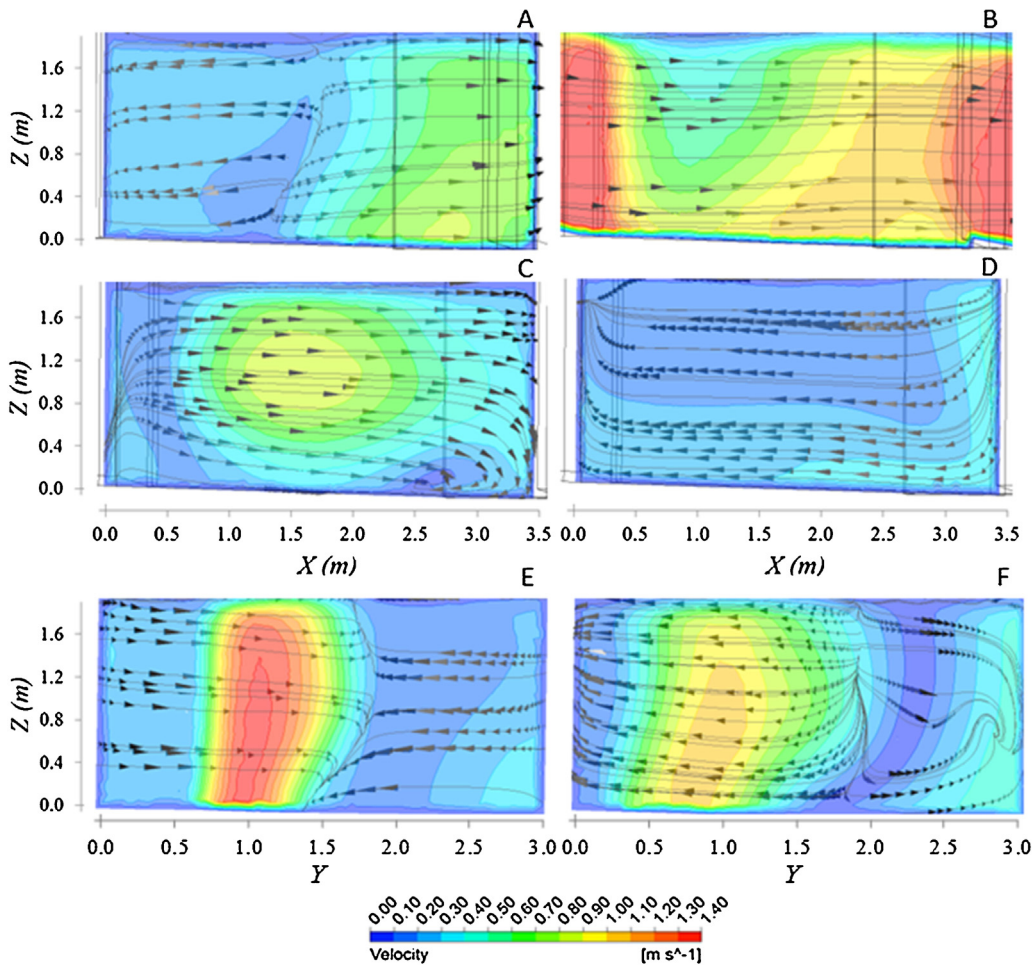


Fig. 11. Spatial variations of velocity magnitude and streamlines along four longitudinal vertical sections (A, B, C, and D) and two transverse vertical sections (E and F) in Pool 5 of Scenario 1.

the upstream direction over the section's full length. Downwelling occurs adjacent to the upstream and downstream ends.

Transverse cross sections E and F had similar spatial velocity variations. Both had a prominent jet region over the water column's full height, with lower velocity recirculation zones surrounding the jet region. In E the jet's core was highly concentrated after entering the pool through the upstream slot and velocity magnitudes decay rapidly away from the concentrated core. E had a maximum velocity of 1.4 m/s in the jet core. In F the jet has grown laterally and its' maximum velocity had decayed in comparison with E. Here, the maximum velocity was 1.10 m/s.

3.4. Kinetic energy and dissipated power

The mean flow kinetic energy per unit mass, K , is described as;

$$K = \frac{1}{2}(U^2 + V^2 + W^2) \quad (3)$$

where, V is the time-averaged velocity in the transverse direction. As shown in Fig. 12, the non-dimensional kinetic energy, $K^{0.5}/U_{sm}$, in pools 5 and 15 was maximum downstream of the slot entrance. Kinetic energy then dissipated rapidly as jet velocity decays as it travelled through the pool. The rapid decay was caused by entrainment of recirculating flow on either side of the jet. Away from the jet area, $K^{1/2}$ was typically less than 35% of U_{sm} in the rest of the pool. The pools at the site fishway had less kinetic energy dissipation as compared to results found by Liu et al. (2006) in a laboratory study of regular pools. This is because the regular pools at the site fishway

were shorter and narrower than pools following the recommended design dimensions. In the shorter and narrower pools less energy decay occurs which produced higher kinetic energy than in pools of recommended design.

Average volumetric energy dissipation rate ($\bar{\epsilon}$) in the pool is calculated using $\bar{\epsilon} = \rho g Q \Delta h / (bh)$, where ρ is the water density, and Q was calculated as $U_{sm} b_0 h$. An average Q equal to $1.63 \text{ m}^3/\text{s}$ was calculated across the pools measured, see Table 3. The estimated $\bar{\epsilon}$ in pools 5, 13 and 15 was about 130 , 60 and 30 W/m^3 , respectively. According to Marriner et al. (2014), the estimated $\bar{\epsilon}$ was 29 W/m^3 in the turning pool. Volumetric energy dissipation is generally considered acceptable if $\bar{\epsilon} < 200 \text{ W/m}^3$ for salmonids, and if $\bar{\epsilon} < 150 \text{ W/m}^3$ for cyprinids (Larinier, 2002). For American/Allis shad and weaker riverine species, Larinier (2002) suggested $\bar{\epsilon}$ should be less than 150 W/m^3 .

4. Fishway design evaluation

Fishway hydrodynamics were investigated for Scenarios 1–5 using CFD modelling to identify the effective regular pool dimensions. In general, when designing for fish passage the first priority is to reduce the maximum velocity such that it is less than the burst speed of ascending fish. Reducing the maximum velocity (maximum head difference between pools) that will in turn result in lower values of turbulence both within the jet and potential resting areas. This reduction also results in lower values in the volumetric dissipated power (Wang et al., 2010). Moreover, having

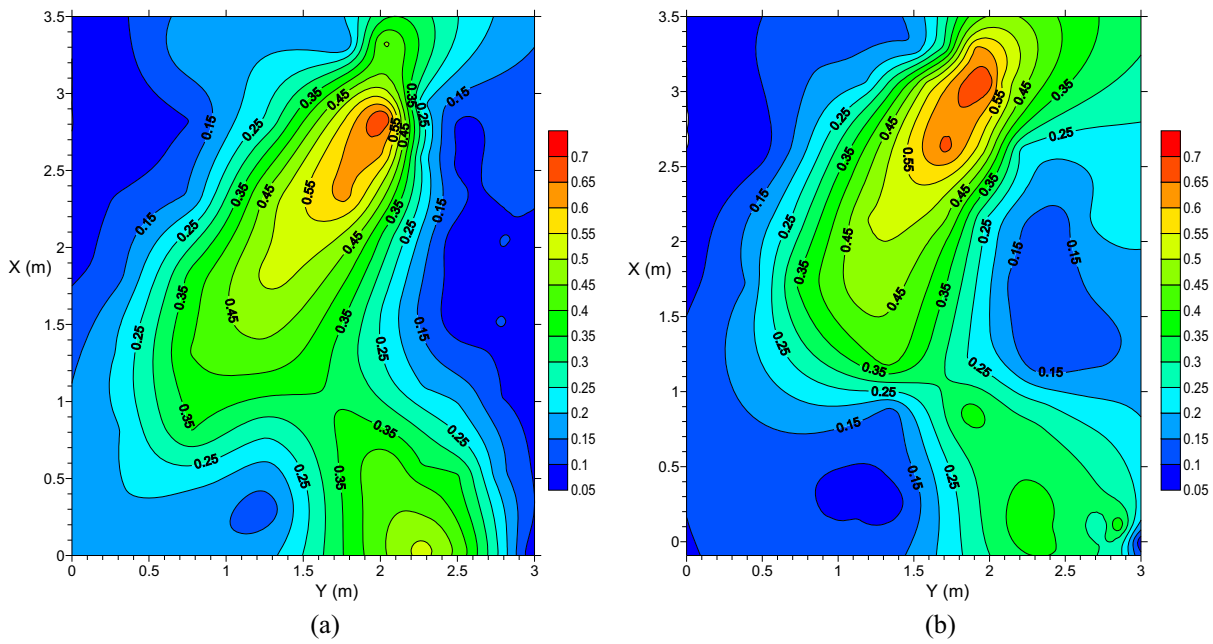


Fig. 12. $K^{0.5}/U_{sm}$ in (a) Pool 5 and (b) Pool 15 of the Vianney-Legendre fishway.

a low-velocity zone (resting zone) in each pool is a key element for fish migration. In a pool, velocity must be kept under 0.30 m/s in 30% to 50% of the pool's volume (Bell, 1986). Wang et al. (2010) concluded that the recommended design ($l = 10b_0$ and $b = 8b_0$) met this criterion for a slope of 5% (36–64% of the volume where velocity < 0.30 m/s). Therefore, designs simulated were evaluated based on slot maximum velocity (U_{sm}) and average volumetric energy dissipation ($\bar{\varepsilon}$). In addition, turbulence parameters (i.e., the maximum turbulent kinetic energy (TKE_m), average energy expenditure per unit distance (E), and maximum momentum of the eddy (Π_m) in fishway pools are important to migrating fish and therefore also important to evaluate (Khan, 2006; Tritico, 2009; Silva et al., 2011).

$TKE_m = \frac{1}{2}(u'^2_{rms} + v'^2_{rms} + w'^2_{rms})$, where u' , v' , w' are the longitudinal, transverse, and vertical fluctuating velocities, respectively. E is estimated from $E = \int_0^S F dS$, where $F = 0.5C_D\rho A_s(U_w - U_f)^2$ is the drag force acting on a fish body, C_D is the drag coefficient, A_s is the wetted surface area of fish, U_w is velocity of flow, and U_f is swimming velocity of fish. Finally the effect of an eddy, impinging on a fish associated with a change in momentum that may cause translational/rotational displacement of the fish, was analyzed to evaluate the pool designs. The maximum momentum of the eddy (Π_m) in the horizontal plane is estimated by $\Pi_m = 0.25\rho\omega_z L_w D$, where A is the integrated area of the eddy, ω_z is the vorticity in horizontal plane, L_w is the fish body width (assuming $L_w = 15$ cm for the lake sturgeon), and D is the eddy diameter equivalent to A (Tritico, 2009).

The predicted fishway hydrodynamics for five different scenarios are summarized in Table 4. Simulated U_{sm} was 1.4, 1.3, 1.2, 1.3, and 1.1 m/s for the Scenarios 1 through 5, respectively. Therefore, U_{sm} was lower than the critical velocity of 2 m/s and the burst swimming speed of 2.52 m/s measured for the white sturgeon (Webber

et al., 2007). At $z = 0.5 h$, TKE_m in the pool was about 0.15, 0.11, 0.08, 0.14, and $0.12 \text{ m}^2/\text{s}^2$ for the Scenarios 1 through 5, respectively.

For the turning pool in this fishway, Marriner et al. (2014) categorized the TKE_m levels as high ($TKE_m > 0.05 \text{ m}^2/\text{s}^2$) in the vertical slots, and low ($TKE_m < 0.05 \text{ m}^2/\text{s}^2$) throughout the remainder of the pool. Comparatively, TKE_m values have been measured at $0.113 \text{ m}^2/\text{s}^2$ in a regular pool (Liu et al., 2006), $0.0676 \text{ m}^2/\text{s}^2$ in a pool-type fishway with offset (i.e., alternating) orifices (Silva et al., 2011), $0.4\text{--}1.2 \text{ m}^2/\text{s}^2$ in a pool type fishway with either a slot or an orifice (Guiny et al., 2005), and $0.6 \text{ m}^2/\text{s}^2$ in a culvert retrofitted with baffles for fish passage (Morrison et al., 2008). The average volumetric energy dissipation rate ($\bar{\varepsilon}$) through Scenarios 1–5, was 149, 93, 74, 59, and 44 W/m^3 , respectively (Table 4).

The variations in average energy expenditure per unit distance (\bar{E}) for the sturgeon at different scenarios were investigated in this study. Assuming a fish passage path at depths of $0.5 h$ for scenarios 1 through 5 (Fig. 6a). The fork length of the sturgeon 1.213 m (Thiem et al., 2011), and its constant burst swimming speed $U_f = 2.52 \text{ m/s}$ (Webber et al., 2007) were used. Khan (2006) used a similar computational procedure for determining energy expenditures by salmon for a vertical slot fishway. E for Scenarios 1 through 5 was 10.2, 7.3, 6.9, 7.4, and 6.6 J/m , respectively (Table 4). Comparatively, \bar{E} has been estimated from 5.4 to 7.6 J/m for the salmon *Oncorhynchus* spp. in a vertical slot fishway by Khan (2006).

In this study, A and ω_z were estimated from the simulated results to estimate the maximum momentum of the eddy (Π_m). The estimated Π_m was 6786, 5975, 10,118, 10,795, and $13,124 \text{ kg.m/s}$ for scenarios 1 through 5, respectively (Table 4). Note that there is a correlation between eddy size and fish body length, in terms of how the eddy will affect the swimming capabilities of fish (Tritico and Cotel, 2010; Webb and Cotel, 2010; Silva et al., 2012).

Table 4
Summary of fishway hydrodynamics using CFD simulation for Scenarios 1–5.

Scenarios	$A_m (\text{m}^2)$	$U_{sm} (\text{m/s})$	$TKE_m (\text{m}^2/\text{s}^2)$	$\bar{\varepsilon} (\text{W/m}^3)$	$\bar{E} (\text{J/m})$	$\omega_z (\text{s}^{-1})$	$\Pi_m (\text{kg m/s})$
1	4.81	1.4	0.15	149	10.2	5.1	6786
2	7.92	1.3	0.11	93	7.3	5.3	5975
3	12.22	1.2	0.08	74	6.9	5.0	10118
4	11.01	1.3	0.14	59	7.4	5.0	10795
5	19.25	1.1	0.12	44	6.6	4.9	13124

Therefore, based on lowest values of maximum slot velocity, maximum turbulent kinetic energy, average volumetric energy dissipation rate, and average energy expenditure per unit distance, Scenario 5 ($l=10b_0$ and $b=8b_0$) was the optimal alternative in comparison to Scenarios 1, 2, and 4. Scenario 5 was also the recommended design by [Bell \(1973\)](#), [Larinier et al. \(1999\)](#), and [Rajaratnam et al. \(1992a,b\)](#), based on overall hydraulic performance and simplicity in construction. It is noted that the longer pool length in Scenario 5 caused the maximum momentum of the eddy to be high. Scenario 3 was the 2nd choice because it had the 2nd lowest values of the above parameters. Scenarios 3 and 5 demonstrate that longer pool lengths provide better overall hydrodynamics for fish passage in comparison to the shorter length or greater pool width.

5. Conclusions

This paper presented the results of a field and numerical study investigating the overall hydraulics of the Vianney-Legendre vertical slot fishway on the Richelieu River in Quebec, Canada. The Vianney-Legendre fishway has a number of unique engineering design elements (i.e.: turning pools, low overall slope, and non-optimal regular pool dimensions) and annually passes approximately 35 species. Moreover, it is one of a very few fishways worldwide to have demonstrated passage of sturgeon ([Thiem et al., 2011](#)).

The fishway was found to have non-uniform flow with an M1 type backwater curve, which is characterized by increasing water levels towards the downstream end of the fishway. At the site, the flow rate and water surface profile were predicted using $Q = C_d \sqrt{2g\Delta h} * (b_0 h)$ under different tailwater levels. Herein, $C_d = 0.86$ for the pools 1–7 under near uniform flow condition was very close to the lower bound of recommended C_d values (0.87–0.90). Flow conditions were non-uniform from pools 8 to 16, where $C_d = 0.95$ was slightly higher than the upper bound of recommended values. C_d at the site fishway was greater than the 0.6–0.8 calculated by [Rajaratnam et al. \(1986\)](#) in a Design 1 regular pool.

The flow pattern in regular pools 5 and 15 was similar to the principal flow pattern. The flow patterns in turning pools were highlighted by a large recirculation area, where the jet did not enter through the pool's centre due to the asymmetric geometry and there were two flow recirculation eddies sitting on either side of the jet. The field results showed that the measured maximum velocity (U_{sm}) in the core of the jet in both regular and turning pools was very close to $U_{theor} = \sqrt{2g\Delta h}$. Velocity was fairly uniform in the top 1.0 m of the pool, below which velocity decays with depth towards the pool floor. The maximum vertical velocity was about 23% and 26% of U_{sm} in pools 5 and 15, respectively. The corresponding values in the turning pools 8 and 13 were about 10% of U_{sm} .

A computational fluid dynamics (CFD) model study was used to examine the detailed flow field in the regular pool. The simulated results demonstrated two distinct flow patterns occurred for $l/b < 1.1$ and $l/b > 1.3$, respectively, and an apparent transition between two patterns took place for a l/b ratio of approximately 1.2. The jet velocity decay in all five scenarios was more rapid than in a plane turbulent jet. Subsequently, the velocity decayed faster in the turning pool as compared to a regular pool.

The numerical model study evaluated the performance of various regular pool geometries. Based on lowest values of maximum slot velocity, maximum turbulent kinetic energy, average volumetric energy dissipation rate, and average energy expenditure per unit distance, Scenario 5 ($l=10b_0$ and $b=8b_0$) was the optimal design alternative to Scenarios 1–4. Scenario 5 was also recommended in previous studies.

It is important to note that the regular pool dimensions at the site fishway were not hydraulically optimal. Yet, in spite of this the site fishway was successful in terms of fish passage, demonstrating

some design flexibility. The overall low slope overcame the non-optimal regular pool design dimensions and produced a fishway with hydraulics suitable to fish passage, as evidenced by the passage success rates and number of species that pass annually. The site fishway was more compact in design, more economical to build, and has been proven to successfully pass multiple species of fish. Further study is needed to optimize the trade-off between economics and hydraulics in this and other vertical slot designs.

Acknowledgements

The authors thank Chris Krath of the University of Alberta, Jason Thiem and Travis Raison of Carleton University for their field assistance. The authors would also like to thank the staff of Ministere des Ressources Naturelles et de la Faune du Quebec, and Parks Canada (2010) at the Saint Ours dam for their contributions to the field study. This project was funded by the NSERC HydroNET research network.

References

- Baki, A.B.M., Zhu, D.Z., Rajaratnam, N., 2014a. [Mean flow characteristics in a rock-ramp-type fish pass](#). *J. Hydraul. Eng.* **140** (2), 156–168.
- Baki, A.B.M., Zhu, D.Z., Rajaratnam, N., 2014b. [Turbulence characteristics in a rock-ramp-type fish pass](#). *J. Hydraul. Eng.* **141** (2), 04014075.
- Bell, M.C., 1973. [Fisheries Handbook of Engineering Requirements and Biological Criteria](#). U.S. Army Corps of Engineers, North Pacific Division, Portland, OR.
- Bell, M., 1986. [Fisheries Handbook of Engineering Requirements and Biological Criteria – Fish Passage Development and Evaluation Program](#). US Army Corps of Engineers, North Pacific Division Portland, OR.
- Bombac, M., Norazd, N., Rodic, P., Cetina, M., 2014. [Numerical and physical model study of a vertical slot fishway](#). *J. Hydrol. Hydromech.* **62** (2), 150–159.
- Cea, L., Pena, L., Puertas, J., Vazquez-Cendon, M.E., Pena, E., 2007. [Application of several depth-averaged turbulence models to simulate flow in vertical slot fishways](#). *J. Hydraul. Eng.* **133** (2), 160–172.
- Chow, V.T., 1959. [Open-Channel Hydraulics](#). McGraw-Hill Book Co., New York, NY, pp. 680.
- Clay, C.H., 1961. [Design of Fishways and Other Fish Facilities](#). Dept. of Fisheries of Canada, Ottawa, pp. 301.
- COSEWIC (Committee on the Status of Endangered Wildlife in Canada). Wildlife Species search. Government of Canada. Updated: 2012/08/03, accessed: 2012/12/05. (1) <http://www.cosewic.gc.ca/eng/sct1/SearchResult.e.cfm?commonName=lake+sturgeon&scienceName=&Submit=Submit>. (2) <http://www.cosewic.gc.ca/eng/sct1/SearchResult.e.cfm?commonName=copper+redhorse&scienceName=&Submit=Submit>.
- Desrochers, D., 2009. [Validation de l'efficacité de la passe migratoire Vianney-Legendre au lieu historique national du canal de Saint-Ours – saison 2008](#). Milieu Inc pour Parcs Canada, Québec, Canada, 47 pp. + 3 annexes.
- Guiny, E., Ervine, D., Armstrong, J., 2005. [Hydraulic and biological aspects of fish passes for Atlantic salmon](#). *J. Hydraul. Eng.* **131** (7), 542–553.
- Hatry, C., Binder, T.R., Thiem, J.D., Hasler, C.T., Smokorowski, K.E., Clarke, K.D., Katopodis, C., Cooke, S.J., 2013. [The status of fishways in Canada: trends identified using the national CanFishPass database](#). *Rev. Fish Biol. Fish.* **23**, 271–281.
- Katopodis, C., Kells, J.A., Acharya, M., 2001. [Nature-like and conventional fishways: alternative concepts?](#) *Can. Water Resour. J.* **26**, 211–232.
- Katopodis, C., Williams, J.G., 2012. [The development of fish passage research in a historical context](#). *Ecol. Eng.* **48**, 8–18.
- Khan, L.A., 2006. [A three-dimensional computational fluid dynamics \(CFD\) model analysis of free surface hydrodynamics and fish passage energetics in a vertical-slot fishway](#). *N. Am. J. Fish. Manage.* **26**, 255–267.
- Larinier, M., Gosset, C., Porcher, J.P., Travade, 1999. [Passes à poissons: Expertises et conception des ouvrages de franchissement](#). La Documentation Française, Paris, France.
- Larinier, M., 2002. [Chapter 5: Pool fishways, pre-barrages, and natural bypass channels](#). *Bull. Fr. Peche Piscic.* **364** (Suppl.), 54–82.
- Liu, M., Rajaratnam, N., Zhu, D.Z., 2006. [Mean flow and turbulence structure in vertical slot fishways](#). *J. Hydraul. Eng.* **132** (8), 765–777.
- Marriner, B.A., Baki, A.B.M., Zhu, D.Z., Thiem, J.D., Cooke, S.J., Katopodis, C., 2014. [Field and numerical assessment of turning pool hydraulics in a vertical slot fishway](#). *Ecol. Eng.* **63**, 88–101.
- Ministère du Développement durable, de l'Environnement, de la Faune et des Parcs (MDDEP). Centre D'expertise hydrique. Updated: 18/03/2013, accessed: 18/03/2013. (1) [http://www.cehq.gouv.qc.ca/suivihydro/graphique.asp?NoStation=030401.\(2\)http://www.cehq.gouv.qc.ca/suivihydro/graphique.asp?NoStation=000116](http://www.cehq.gouv.qc.ca/suivihydro/graphique.asp?NoStation=030401.(2)http://www.cehq.gouv.qc.ca/suivihydro/graphique.asp?NoStation=000116).
- Morrison, R., Hotchkiss, R., Stone, M., Thurman, D., Horner-Devine, A., 2008. [Turbulence characteristics of flow in a spiral corrugated culvert fitted with baffles and implications for fish passage](#). *Ecol. Eng.* **35**, 381–392.
- Nortek AS, 2011. [Vectrino velocimeter user guide](#). Nortek AS, Vangkrogen, Norway.

- Parks Canada, 2010. Vianney-Legendre Fishway at the Saint-Ours Canal National Historic Site of Canada, <http://www.pc.gc.ca/lhn-nhs/qc/saintours/ne.aspx> (Updated: 18/08/2010, accessed: 05/2011).
- Peake, S., Beamish, F.W., McKinley, R.S., Scruton, D.A., Katopodis, C., 1997. Relating swimming performance of lake sturgeon, *Acipenser fulvescens*, to fishway design. *Can. J. Fish. Aquat. Sci.* 54 (6), 1361–1366.
- Perez, J.F.F., Ronda, F.J.S., Paredes, A.M.A., Vega, A.G., 2014. Modeling water-depth distribution in vertical slot fishways under uniform and non-uniform scenarios. *J. Hydraul. Eng.* 140 (10), 60614016–6014025.
- Puertas, J., Cea, L., Bermudez, M., Pena, L., Rodriguez, A., Rabunal, J.R., Balairon, L., Lara, A., Aramburu, E., 2012. Computer application for the analysis and design of vertical slot fishways in accordance with the requirements of the target species. *Ecol. Eng.* 48, 51–60.
- Rajaratnam, N., Amsterdam, The Netherlands 1976. *Turbulent Jets*.
- Rajaratnam, N., Van der Vinne, G., Katopodis, C., 1986. Hydraulics of vertical slot fishways. *J. Hydraul. Eng.* 112, 909–927.
- Rajaratnam, N., Katopodis, C., Paccagnan, R., 1992a. Field studies of fishways in Alberta. *Can. J. Civ. Eng.* 19, 627–638.
- Rajaratnam, N., Katopodis, C., Solanki, S., 1992b. New designs for vertical slot fishways. *Can. J. Civ. Eng.* 19, 402–414.
- Schlumberger Water Services, 2011. *Mini-Diver Product Manual*. Schlumberger Water Services, Delft, The Netherlands.
- Silva, A.T., Katopodis, C., Santos, J., Ferreira, M., Pinheiro, A., 2012. Cyprinid swimming behavior in response to turbulent flow. *Ecol. Eng.* 44, 314–328.
- Silva, A.T., Santos, J.M., Ferreira, M.T., Pinheiro, A.N., Katopodis, C., 2011. Effects of water velocity and turbulence on the behaviour of Iberian barbell (*Luciobarbus bocagei*, Steindachner 1864) in an experimental pool-type fishway. *River Res. Appl.* 27, 360–373.
- Thiem, J., Binder, T., Dawson, J., Dumont, P., Hatin, D., Katopodis, C., Zhu, D.Z., Cooke, S., 2011. Behaviour and passage success of upriver-migrating lake sturgeon *Acipenser fulvenscens* in a vertical slot fishway on the Richelieu River, Quebec, Canada. *Endanger. Species Res.* 15, 1–11.
- Thiem, J.D., Binder, T.R., Dumont, P., Hatin, D., Hatry, C., Katopodis, C., Stamps, K.M., Cooke, S.J., 2013. Multispecies fish passage behaviour in a vertical slot fishway on the Richelieu River, Quebec Canada. *River Res. Appl.* 29, 582–592.
- Tritico, H.M., (PhD dissertation) 2009. *The Effects of Turbulence on Habitat Selection and Swimming Kinematics of Fishes*. University of Michigan, Ann Arbor.
- Tritico, H.M., Cotel, A.J., 2010. The effects of turbulent eddies on the stability and critical swimming speed of creek chub (*Semotilus atromaculatus*). *J. Exp. Biol.* 213, 2284–2293.
- Warren, J.J., Beckman, L.G., 1993. Fishway Use by White Sturgeon on the Columbia River. Washington Sea Grant Program, Marine Advisory Services.
- Wang, R.W., David, L., Larinier, M., 2010. Contribution of experimental fluid mechanics to the design of vertical slot fish passes. *Knowl. Manag. Aquat. Ecosyst.* 396 (02), 1–21.
- Wateroffice Canada, 2015. Daily Discharge Graph for RICHELIEU (RIVIERE) AUX RAPIDES FRYERS (02OJ007). <https://wateroffice.ec.gc.ca/report/report.e.html?mode=Graph&type=h2oArc&stn=02OJ007&dataType=Daily¶meterType=Flow&year=2014&y1Mean=1&scale=normal> (updated 13.08.15, accessed 08.11.15).
- Webb, P.W., Cotel, A.J., 2010. Turbulence: does vorticity affect the structure and shape of body and fin propulsors? *Integr. Comp. Biol.* 50 (6), 1155–1166.
- Webber, J.D., Chun, S.N., MacColl, T.R., Mirise, L.T., Kawabata, A., Anderson, E.K., Sung Cheong, T., Kavvas, L., McGee Rotondo, M., Hochgraf, K.L., Churchwell, R., Cech Jr., J.J., 2007. Upstream swimming performance of adult white sturgeon: effects of partial baffles and a ramp. *Trans. Am. Fish. Soc.* 136, 402–408.
- Wu, S., Rajaratnam, N., Katopodis, C., 1999. Structure of flow in vertical slot fishway. *J. Hydraul. Eng.* 125 (4), 351–360.